KEYNOTE ARTICLE

Environmentally Friendly Chemistry using Supported Reagent Catalysts: Structure–Property Relationships for Clayzic

James H. Clark,*[a] and in part Stephen R. Cullen,[a] Simon J. Barlow[b] and Tony W. Bastock[b]
[a] *Department of Chemistry, University of York, Heslington, York, UK YO1 5DD*
[b] *Contract Chemicals Ltd., Knowsley Industrial Park, Prescot, Merseyside, UK L34 9HY*

Supported reagents have been widely used in organic synthesis for some 25 years and their importance is likely to increase as a result of new environmental legislation and the drive towards clean technology. While many supported reagents are stoichiometric in reactions the successful development of genuinely catalytic materials greatly enhances their value especially in liquid phase, typically fine chemical syntheses. Achieving an understanding of the nature of these fascinating materials is also an important aspect of their development and is essential if their true potential is to be realised. Solid acids are the most widely studied of supported reagents and their use as more environmentally acceptable replacements for conventional Brönsted and Lewis acids is likely to become increasingly important. Clayzic is a good example of an environmentally friendly catalyst with particular value as an alternative to the hazardous reagent aluminium chloride in Friedel–Crafts reactions. The structure and properties of this catalyst are, however, poorly understood. X-Ray diffraction studies show that thermal treatment of either clayzic or its base material K10 results in the loss of any montmorillonite crystallinity that remained after the acid treatment of tonsil 13 used to form K10. Thermal treatment of clayzic also results in a steady increase in the surface area of the material. While this is also consistent with structural changes the increase is also likely to be partly due to the dehydration allowing the non-polar adsorbate to enter more of the polar regions of the material. These polar regions can be identified as mesopores created by the acid treatment of the clay and in which the zinc ions largely reside. Spectroscopic titration of the acid sites in clayzic show these to be largely Lewis acid in character. Thus clayzic owes its remarkable Friedel–Crafts activity to the presence of high local concentrations of zinc ions in structural mesopores. Relative reaction rates for the clayzic catalysed benzylation of alkylbenzenes also reveal the importance of these highly polar mesopores. Considerable rate enhancements can be achieved by thermally activating the catalyst and this can be largely attributed to the dehydration of the catalyst enabling better partitioning of the alkylbenzenes into the mesopores. Clayzic can be considered as being a large pore molecular sieve but where the sieving of molecules is controlled more by molecular polarities/polarisibilities than by molecular shape.

Environmentally Friendly Catalysis

One important consequence for chemistry of new environmental legislation and the drive towards 'Clean Technology' will be the use of 'Environmentally Friendly Catalysis', typically involving the use of solid catalysts. Their use should lead to minimal pollution and waste and should themselves be environmentally benign. The use of such catalysis in the manufacture of fine chemicals and chemical intermediates, processes that normally operate in the liquid phase, and in which heterogeneous catalysis has traditionally been little used, is likely to be especially important in the future. Supported reagents should have an important role to play in this context.[1]

Supported reagents based on inorganic materials have been known for some 25 years and the development of the subject is witnessed by the steady increase in the number of articles on the subject and by the recent appearance of several books.[2–4] The 1990s have also seen the first international symposia on supported reagent chemistry and the first industrial applications of supported reagent catalysts.[1] This rate of development can only be enhanced by environmental legislation which is placing increasing demands on the chemical industry to replace outdated chemical processes with new cleaner methods and thus reduce pollution at source.

Early research work on supported reagent chemistry at York, as elsewhere, largely involved stoichiometric reagents such as supported cyanides (*e.g.* KCN–F-alumina for the conversion of alkyl halides to alkyl cyanides), supported oxidants (*e.g.* $KMnO_4$–silica for the selective conversion of primary alcohols to aldehydes) and supported Cu^I reagents (*e.g.* CuI–charcoal for the conversion of aryl bromides to aryl iodides). Truly catalytic supported reagents are required however if the materials are to find widespread use in chemical processes.

Supported Fluorides[4]

Ironically, one of the first significant, truly catalytic supported reagents, KF–alumina, emerged from research aimed at designing more reactive sources of F^- for nucleophilic fluorination, *i.e.*, stoichiometric supported reagents. Evaporation of a slurry of alumina and aqueous KF (typically adjusted to give a final material of loading 1–2 mmol KF g^{-1} alumina) gives a free flowing particulate solid which shows useful basic activity in a wide range of organic reactions including Aldol and Knoevenagel condensations, alkylations and Michael reactions (Fig. 1).

In many of these reactions the supported reagent is genuinely

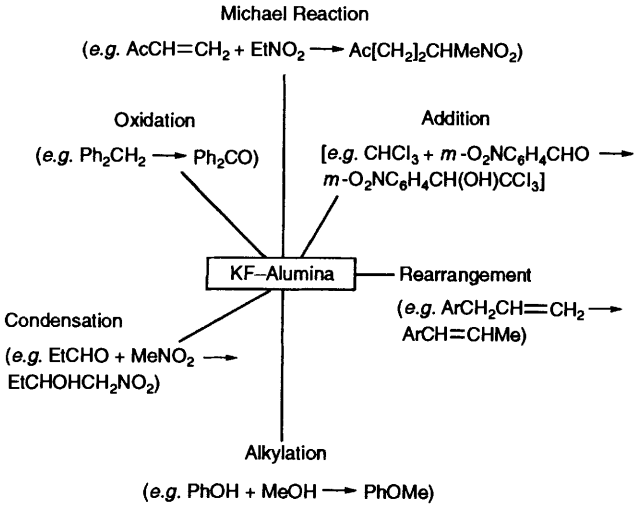

Fig. 1 Some reactions catalysed by KF–alumina[4]

X-Ray Diffraction	—Absence of salt pattern at 2 mmol g^{-1} —KF and K_3AlF_6 evident at 10 mmol g^{-1} —KX evident after reaction with RX
Thermogravimetric Analysis	—Major weight loss at 45–100 °C —Slow additional weight loss up to 500 °C
Infrared Analysis	—Formation of K_3AlF_6 ($KAlF_4$?) —Indication of strong OHF^- hydrogen-bonding? —Formation of CO_3^{2-}
Surface Area Analysis	—Material destruction proportional to loading and activation temperature
High Resolution Solids NMR Spectroscopy	—Coordinatively unsaturated F^-
Fast Atom Bombardment Mass Spectrometry	—Clustering of salt at high loadings

Fig. 2 Analytical studies on KF–alumina[4]

catalytic but in others, more than stoichiometric quantities of fluoride are required. Reactions that produce hydrogen halide such as alkylations employing alkyl halides fall into the latter category. This can be explained by consideration of the following equations.

$$RZH + F^- \longrightarrow RZH \cdots F^- \longrightarrow RZ^- + HF$$

$$RZ^- + R'X \longrightarrow R'ZR + X^-$$

$$HF + F^- \longrightarrow FHF^- \text{ (stable)}$$

Overall

$$RZH + R'X + 2F^- \longrightarrow R'ZR + FHF^- + X^-$$

Interestingly, reactions that produce water such as Aldol condensations, only require catalytic quantities of the supported fluoride. Fluorides are not destroyed by water although hydration can reduce activity. This is in contrast to many bases such as hydrides, amides, and alkoxides, that are irreversibly destroyed by water.

Supported fluorides and KF–alumina in particular, are among the best studied and most frequently employed supported reagents. One perplexing aspect of their chemistry is the variability in their activity as solid base catalysts. Supported fluorides have been variously described as weak, moderate, strong and even super-bases.[4] In an attempt to understand this complex behaviour we have carried out extensive analytical studies on KF–alumina in particular (see Fig. 2). The major conclusions of these investigations are that:

(*i*) several different species may be present on the surface of supported fluorides including F^-, AlF_4^-, AlF_6^{3-}, OH^-, O^{2-} and CO_3^{2-}; and

(*ii*) the basicity of the material will depend on the relative concentrations of the basic species which are controlled by the loading of the fluoride and the activation of the supported reagent.

Studies on supported fluorides taught us the importance of employing analytical techniques to learn more about the nature of supported reagents and the dependence of their properties on the method of preparation. This has proven invaluable in the development of new supported reagents.

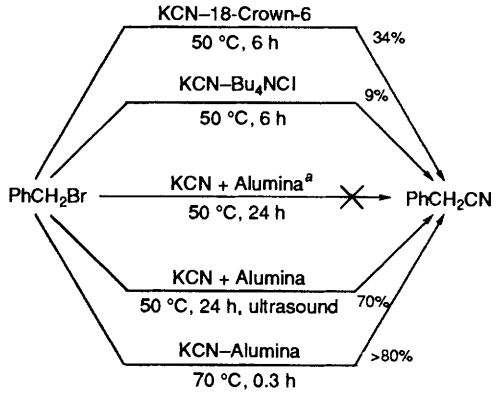

Fig. 3 Relative reactivities of KCN reagents ([a] 9% Ph_2CH_2 using PhH as solvent)

Supported Cyanides[4]

Infrared spectroscopic analysis especially *via* the use of diffuse reflectance techniques (enabling direct analysis of powdered samples) has proven to be invaluable to the study of several interesting supported reagents. Supported cyanides, with $\nu_s(C{\equiv}N)$ bands occurring in such a quiet region of the IR spectrum, were obvious candidates. We were able to fully optimise the efficiency of, and explain the variations in the activity of supported cyanides by monitoring the band position and shape in their IR spectra. The most active supported reagent, KCN supported on fluorinated alumina, at a loading of *ca.* 1 mmol g^{-1} is significantly more reactive than analogous KCN–crown ether and KCN–phase transfer catalysts (Fig. 3). Significantly it is also more active than an intimate mixture of KCN and alumina, even under conditions of ultrasonic activation—clearly the effort involved in optimising conditions for and preparing the actual supported reagent is rewarded by increased activity. We were then able successfully to extend our research and methods to include supported CuCN (and from there to other supported Cu^I nucleophilic reagents) which is a valuable reagent for aromatic cyanations ($ArX \longrightarrow ArCN$). Supported cyanides are stoichiometric reagents at best although it should be possible to reuse the material after reactivation with fresh cyanide.

Solid Oxidant Supported Reagents[1,4,5]

Solid oxidants based on silica, alumina and other porous materials are another important class of supported reagents.

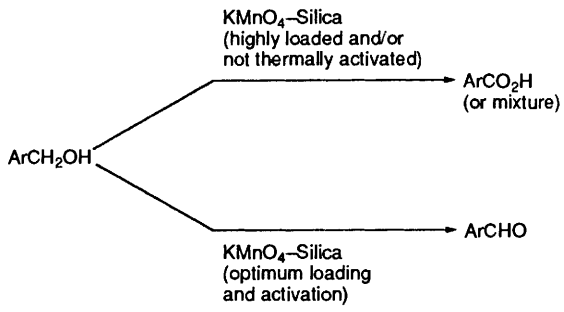

Fig. 4 Reaction of benzyl alcohol with supported $KMnO_4$

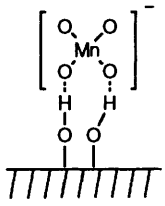

Fig. 5 Possible orientation of MnO_4–physisorbed on silica[6]

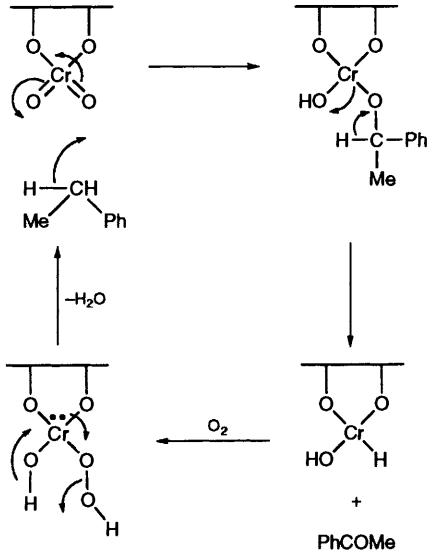

Fig. 6 Possible mechanism for the reaction of chemisorbed $Cr_2O_7^{2-}$ on alumina with an alkylaromatic substrate

Our early research in this area was again restricted to stoichiometric materials. Nonetheless we were again able to use IR spectroscopy to help to optimise $KMnO_4$–silica for example, as an oxidant. Remarkably, it proved possible to 'tune' this reagent so that it reacted with benzyl alcohols to selectively give the aldehyde rather than the acid (Fig. 4). We interpreted the IR spectrum of the form of $KMnO_4$–silica that selectively gave the aldehyde, as being due to the physisorbed permanganate sitting on the surface with two of the oxygens interacting with the surface and hence creating a pseudo C_{2v} symmetry as opposed to the normal T_d symmetry for MnO_4^- (Fig. 5).[6] This observation proved to be important several years later when we sought to develop truly catalytic supported reagent oxidants.

Treatment of alumina with aqueous $KMnO_4$ or $K_2Cr_2O_7$ under carefully controlled conditions leads to genuinely catalytic oxidants that are capable of selectively oxidising alkylaromatics at atmospheric pressure using only air as the source of oxygen. Furthermore, the reactions can be run in the absence of solvent when the substrate is a liquid. Remarkably high catalytic turnover efficiencies can be achieved. In a typical experiment over 50% conversion of 1 mol of the neat substrate can be accomplished using only 1 g of the chromium-containing catalyst. The actual concentration of active (chromium or manganese) sites on the surface of the supported reagents is very low (< 0.1 mmol g^{-1}), well below the normal reagent loadings for supported reagents (1–10 mmol g^{-1}) and below the values we have calculated for monolayer coverage. The catalytic forms of supported permanganate and dichromate are unaffected by water which leads us to believe that the metal is fixed to the surface of the support by aluminium–oxygen–chromium bonds (Fig. 6), reminiscent of the stoichiometric silica–permanganate reagent we had studied several years earlier (Fig. 5). The very low loading of chromium or manganese has prevented us from properly characterising the surfaces of these supported reagents although we hope to be able to report further on these remarkable oxidants at a later date.

Solid Acid Supported Reagents[1–4]

While the use of solid bases, solid oxidants and to an extent, stoichiometric (typically nucleophilic) supported reagents represent important examples of environmentally friendly chemical reactions, we, along with many other groups have spent a significant amount of time studying solid acid supported reagents. This can be justified when one considers the enormous range of acid catalysed reactions (including some of the most important chemical processes such as cracking, alkylation and isomerisation) and the hazards and other environmental drawbacks associated with the use of traditional acidic reagents.

There are a very large number of known and well studied solid acids. Of these zeolites (aluminosilicate molecular sieves) are certainly the best known. Their ease of handling and use, robustness, catalytic activity and remarkable shape selectivity makes them excellent candidates for environmentally friendly catalysts. Unfortunately while they are very effective catalysts in many vapour phase processes, slow diffusion through their microporous structures makes them relatively poor catalysts in the liquid phase. Larger pore molecular sieves (including aluminophosphates) offer greater potential for liquid phase catalysis and promising results have been obtained recently in several areas including general acid catalysis and asymmetric synthesis. We have concentrated our efforts on mesoporous solid acid supported reagents as catalysts for typically acid-catalysed liquid phase processes. Of these processes, the most important, diverse and challenging are Friedel–Crafts reactions.

The Friedel–Crafts reaction is probably the most important 'named' reaction in organic chemistry. Aryl alkylations, acylations, benzoylations and sulfonylations all fall under this heading, and the range of products derived from these reactions cover cosmetics, pharmaceuticals, plastics and paper products. Traditional Friedel–Crafts processes employ mineral acids such as HF and H_2SO_4, or Lewis acids such as $AlCl_3$ and BF_3. Of these, the most widely used catalyst in liquid phase batch processes is $AlCl_3$. While $AlCl_3$ is readily available and inexpensive, it has numerous drawbacks including:

(*i*) it is violently decomposed by water, liberating 3 mol equiv. HCl;

(*ii*) it is corrosive and dangerous to handle;

(*iii*) it gives poor selectivity in alkylation reactions causing polyalkylated and isomerised by-products;

(*iv*) it is required in greater than stoichiometric quantities for acylations, benzoylations and sulfonylations due to its complexation of product molecules; and

(*v*) decomposition of product complexes requires addition to water which is highly exothermic, liberates large volumes of gaseous effluent (HCl) and creates an organic-contaminated,

aluminium rich, acidic aqueous effluent which is increasingly expensive and difficult to deal with.

These drawbacks become major disadvantages in times of environmental concern and alternatives to $AlCl_3$ must be developed.

Clayzic [1,4,7,8]

Clay based materials have been used as catalysts in liquid phase organic reactions for many years. Early attempts to develop active clay-based catalysts for Friedel–Crafts reactions [9,10] met with limited success but the emergence of zinc chloride supported on acid-treated montmorillonite (K10), 'Clayzic', was a definite breakthrough in the search for environmentally friendly Friedel–Crafts catalysts.[7] Initial screening of various metal reagents supported on the acid-treated montmorillonite clay, K10, revealed that while most reagents reduced the, already low, activity of the acid-treated clay and earlier studies had clearly shown the inferior activity of ion-exchanged materials, supported $CuCl_2$, $NiCl_2$ and $ZnCl_2$ give a definite enhancement in activity. Further studies then focused on K10–$ZnCl_2$ 'Clayzic' which in effectively catalysing benzylations in minutes at room temperature, demonstrated a remarkable synergistic effect between two individually weak Friedel–Crafts catalysts.[7,8,11]

Clayzic has been the subject of over 20 articles since it was first reported in 1989. Unfortunately, there is little consistency in the methods of preparation or activation but its very useful activity, especially in liquid phase Friedel–Crafts alkylations, is beyond question.

Recent studies on clayzic have revealed a number of interesting and important points including:

(*i*) at least some of the active sites in clayzic can be poisoned by oxygenated substrate or product molecules; [12,13]

(*ii*) clayzic contains both Brönsted and Lewis acid sites; [12,14]

(*iii*) there is little residual lamellar structure in the catalysts; [14,15]

(*iv*) the activation temperature for clayzic critically affects its activity in Friedel–Crafts benzylation reactions; [16] and

(*v*) the order of reactivities of halobenzenes in clayzic catalysed Friedel–Crafts benzylations is dependent on catalyst activation.[16]

We have recently completed further studies on clayzic (and in some cases on the K10 support) on structural, spectroscopic and reactivity aspects, that both confirm the above conclusions and help us to build up a picture of this remarkable catalyst and to understand the origin of its activity.[17]

Studies on the Structure of Clayzic

Powder Diffraction Patterns

The powder diffraction pattern of K10 is significantly different to that of its parent clay tonsil 13. Most significantly the basal (001) reflection at $2\theta = 6.0°$ ($d = 14.7$ Å), is not observed. There is also now a sharp and much more intense reflection at $2\theta = 9.0°$ ($d = 9.8$ Å) corresponding to the 2:1 layer structure of montmorillonite. These observations suggest that the lamellar structure of tonsil 13 has been disrupted to such a large extent, by the acid treatment procedure, that not enough crystallinity has been retained for a reflection to be seen in the powder XRD (X-ray diffraction) pattern. Significant 2:1 layer structure appears to have been retained, suggesting that the acid treatment conditions used in producing K10, are relatively mild or that some structure has been preserved, *e.g.* by 'passivation'.[18]

There are significant differences between the diffraction patterns of the calcined (275 °C overnight) and uncalcined samples of K10. Most notably, the reflection at $2\theta = 9.0°$ in the diffraction pattern of uncalcined K10 which corresponds to a *d* spacing of 9.8 Å and is due to remaining 2:1 structure of the montmorillonite, is not present in the diffraction pattern of calcined K10. This suggests that any remaining clay crystallinity has been broken down by the calcination procedure.

The reflections in the diffraction pattern of unactivated K10 which can be assigned to α-quartz ($2\theta = 26.8°$, $d = 3.33$ Å and $2\theta = 21.0°$, $d = 4.23$ Å) appear to be present in the diffraction pattern of calcined K10, although the former reflection does appear to be of significantly diminished relative intensity. In addition, two further reflections appear in the latter pattern, both of which have greater relative intensities than the α-quartz reflections. The first appears at a 2θ angle of 20.7° ($d = 4.28$ Å) and the second at a 2θ angle of 28.0° ($d = 3.18$ Å). Neither of these reflections can be assigned with confidence. It does not appear that these reflections are due to other crystalline forms of silica such as β-quartz, tridymite or crystobalite, which might have been formed from α-quartz by the calcination process. This is consistent with the reported calcination temperatures required for equilibration of silica to other allotropes: 570–870 °C for β-quartz, 870–1470 °C for tridymite and > 1470 °C for crystobalite.[19]

The diffraction patterns for unactivated and activated (275 °C, overnight) clayzic are quite similar at first inspection. The pattern for unactivated clayzic shows a sharp reflection at $2\theta = 9.0°$ (corresponding to a *d* spacing of 9.8 Å) and is most probably due to remaining montmorillonite 2:1 structure. This reflection appears to be present in the pattern obtained for the activated sample ($2\theta = 9.0°$, $d = 9.6$ Å) although it is of much reduced relative intensity. The reflection at $2\theta = 7.9°$ ($d = 4.45$ Å) in the pattern of unactivated clayzic [an (*hk*) clay structure reflection] is also of much reduced relative intensity in the pattern for the thermally activated sample. The pattern obtained for the unactivated sample shows reflections due to the presence of α-quartz at $2\theta = 20.8°$ ($d = 4.26$ Å) and at $2\theta = 26.8°$ ($d = 3.33$ Å). Similar reflections appear in the pattern obtained from the calcined sample at $2\theta = 20.2°$ ($d = 4.38°$) and at $2\theta = 26.9°$ ($d = 3.31$ Å), although it is not clear whether the former reflection is due to α-quartz as its position does not correspond exactly to that in the pattern of the unactivated sample.

The results obtained here and elsewhere suggest that thermal treatment of either clayzic or the support K10 results in the loss of any montmorillonite crystallinity that remained after the acid treatment of tonsil 13 used to form K10. It is also noticeable that significant differences exist between the crystal structure types that exist in calcined clayzic and calcined K10. In particular, the unassigned reflections at $2\theta = 20.7°$ ($d = 4.28$ Å) and $2\theta = 28.0°$ ($d = 3.18$ Å) in the pattern of the calcined K10 are not present in the pattern of thermally activated clayzic. The nature of these differences and the reasons behind them are not clear. These results are also consistent with the observation that structural changes take place within K10 and clayzic on calcination and suggest that little or no crystallinity is developed within clayzic, the material becoming largely amorphous.

Surface Areas and Cation Exchange Capacities

The effect of the acid treatment on the surface area (*a*) and cation exchange capacity (CEC) of tonsil 13, in producing K10, are shown in Table 1. Specific surface areas (*a*) were measured by adsorption of dinitrogen at 77 K and application of the BET isotherm. CECs were determined photometrically by methylene blue adsorption after the method of Robertson and Ward [20] and are in good agreement with results obtained by McCabe.[21]

These data demonstrate that there is a significant decrease in the CEC and an almost five-fold increase in the measured

Table 1 Comparison of cation exchange capacities (CECs) and specific surface areas (*a*) (BET) for the montmorillonite tonsil 13 and its acid treated derivative K10

Material	CEC/mol equiv. 100 g^{-1}	$a/m^2\ g^{-1}$
Tonsil 13	78	47
K10	35	230

surface area, after acid treatment of tonsil 13 to produce K10. These data are consistent with the XRD data in suggesting that extensive delamination of the layered structure of the montmorillonite has occurred in producing K10. This conclusion is in variance with conclusions drawn by Laszlo based on ^{27}Al solid NMR studies that the octahedral layer of K10 has not been significantly perturbed by the acid treatment procedure.[22] The conclusions drawn here are however, in agreement with the findings of Brown and Rhodes, who found that even mild acid treatment of the montmorillonite Carmargo White, severely disrupted both the octahedral layer of the aluminosilicate sheets and the lamellar structure of the mineral.[15]

It is significant that the loading of zinc chloride used in forming clayzic (100–224 mol equiv. 100 g^{-1}, depending on method of preparation) is much greater than the CEC of the support and that clayzic has been shown to be a much more active catalyst towards Friedel–Crafts benzylation reactions than the purely zinc cation exchanged material studied previously by Laszlo and Mathy.[10] We have also found that clayzic prepared using tonsil 13 as the support (tonsil-zic) is a much poorer catalyst for Friedel–Crafts benzylation reactions than Clayzic.[17] These findings suggest that it is not the ordered lamellar structure of the montmorillonite and zinc ions in the exchange cation positions, that are important in clayzic, but that it is the effect of the acid treatment on the ordered layer structure that is responsible for the observed catalytic activity of this material.[23] These observations also imply that the lamellar structure of the clay is not responsible for any observed regioselectivity towards the *para*-position in Friedel–Crafts electrophilic aromatic substitution reactions and that the strength of the electrophile produced by clayzic may be the determining factor.[16]

Brown and Rhodes have shown that there is no correlation between the surface area of the support and the catalytic activity of clayzic-type materials, when using progressively more acid treated Carmargo White and mesoporous silica supports.[14] The effect of thermal activation (by calcination in air) on the specific surface area of clayzic has been investigated and is shown graphically in Fig. 7.

Fig. 7 suggests that there is a linear increase in the specific surface area of clayzic with increasing calcination temperature, in the range studied. This observation is consistent with the catalyst undergoing structural changes with calcination, as was suggested earlier. It is also possible that the dehydrating effect of the calcination procedure may allow the non-polar adsorbate to enter more of the polar regions of the material (*e.g.* the mesopores) and thus allow their contribution to the surface area to be measured. The use of dinitrogen as the adsorbate is known not to measure the surface areas of certain very polar regions (such as the interlayer regions) of clay minerals.[24]

It is interesting to note that no maximum is observed in Fig. 7, as was observed for the effect of calcination temperature on the catalytic activity of clayzic.[16] These results are in agreement with Brown and Rhodes' conclusions that the catalytic activity of the supported reagent is not dependent on the surface area of the formed material and that it is the presence of mesopores within the support that is important to the activity of the

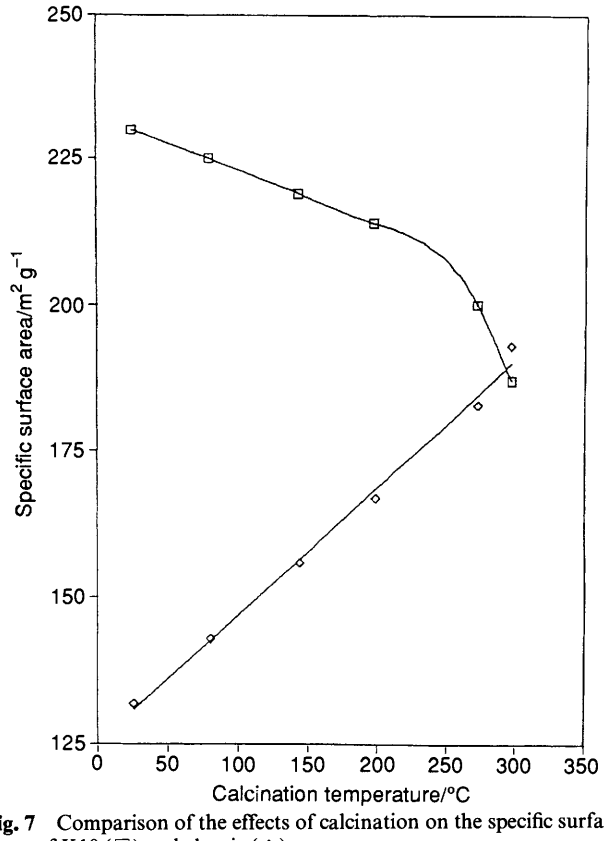

Fig. 7 Comparison of the effects of calcination on the specific surface areas of K10 (□) and clayzic (◇)

catalyst. These results are also in variance with Laszlo's postulate, that the active zinc ion sites reside at the edges of clay platelets.[25] If this were the case, it might be expected that the catalytic activity of clayzic would increase with the surface area of the support and the supported reagent.

The effect of calcination on the surface area of the support material K10 has also been studied and the results are shown alongside those for clayzic in Fig. 7.

The effect of calcination on K10 is in marked contrast to that seen for clayzic, where calcination is seen to significantly increase the measured surface area. This observation supports the suggestion that the increase in measured specific surface area for clayzic is, in part, caused by the effect of dehydration of the catalyst. This may reduce the polarity of certain regions of the material, particularly the highly polar zinc-containing mesopores sufficiently to allow their contribution to the surface area to be measured when using dinitrogen as the adsorbate.

The surface area of clayzic is increasing well after thermogravimetric analysis shows the removal of physisorbed water and this observation, along with other significant differences between K10 and clayzic (including a difference in the optimum activation temperatures)[16] may imply an effect of the zinc ions on the material structure.

Porosities

It has been shown that acid treatment of montmorillonites can result in the formation of mesopores.[14,15,18,26] Pinnavaia has recently reported that K10 is indeed mesoporous with a broad distribution of pore diameters, but with the majority in the 60–100 Å diameter range.[27]

The adsorption–desorption isotherm for K10 has been constructed (using dinitrogen as the adsorbate at 77 K). This has the form of the Type IV isotherm in the Brunauer, Deming, Deming and Teller classification[28] and shows hysteresis

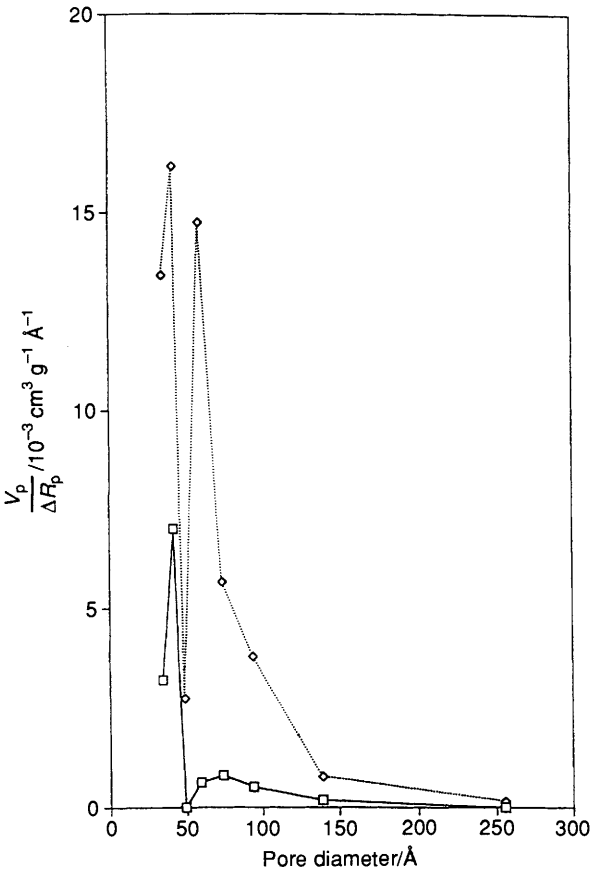

Fig. 8 Comparison of pore size distributions for K10 (◇) and tonsil 13 (□) (R_p = pore radius)

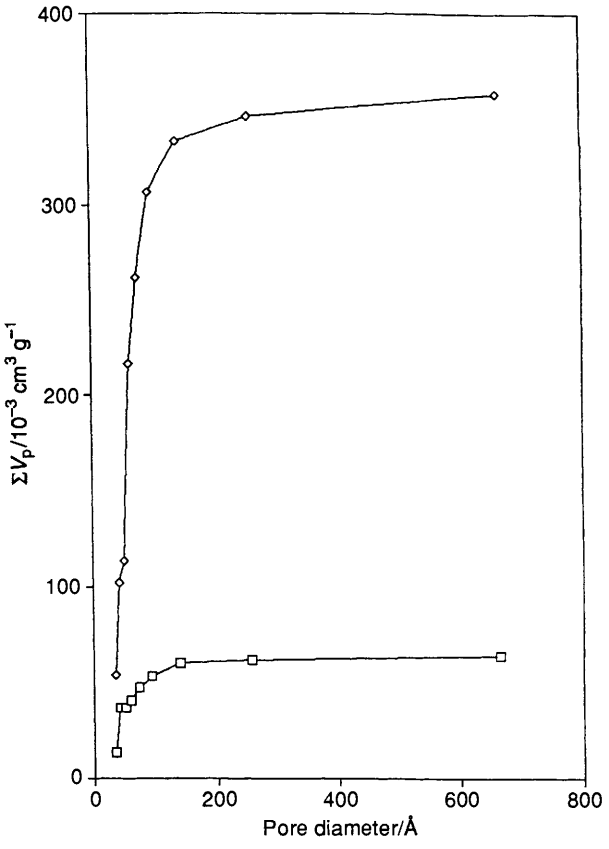

Fig. 9 Comparison of cumulative pore volumes for K10 (◇) and tonsil 13 (□)

between the adsorption and desorption branches, which is characteristic of a mesoporous solid.[29] Furthermore, the shape of the hysteresis loop is of the H3 type in the IUPAC classification[22,30] (formerly Type B in the De Boer classification)[31] and is characteristic of slit shaped mesopores or of adsorbents constituted from plate-like particles.

Considering the delaminated structure of K10 compared to that of tonsil 13, it seems likely that the mesoporous structure of K10 may result from the stacking of plate-like particles, and that these plate-like particles are likely to be the 2:1 layers of the parent clay, which do show a reflection in the powder XRD pattern. These observations are consistent with Pesquera's suggested structure for a montmorillonite after the extent of acid attack has been limited by 'passivation'. Indeed, a similar structure, which has been described as a 'card house', has been suggested for K10 by Onaka and co-workers, although their proposal was only based on surface area and powder XRD evidence.[32] Laszlo has also alluded to this structure for montmorillonites in general.[33] A very similar structure is shown by Gregg and Sing for adsorbates of this type.[29]

The pore size distribution and cumulative pore volumes for tonsil 13 and K10 have been determined and are shown in Figs. 8 and 9 respectively. Fig. 8 shows that tonsil 13 possesses very little porosity in the mesopore range. In comparison, K10 demonstrates significant porosity in the 50–150 Å pore diameter range, with a rather narrow distribution at a maximum of about 65 Å and a much broader distribution appearing as a shoulder between about 70 and 140 Å. The pore size distribution obtained for K10 is in excellent agreement with that reported by Pinnavaia.[27] Both the pore size distribution plots show sharp maxima at about 40 Å, although Gregg and Sing[29] have attributed the appearance of such maxima to an artefact which is due to the condensation of adsorbate in interparticle voids.

Table 2 Comparison of specific surface area and total pore volume (V_p) for tonsil 13 and K10

Material	a/m^2 g^{-1}	V_p/cm^3 g^{-1}
Tonsil 13	47	0.06
K10	230	0.36

Fig. 9 shows that the cumulative pore volume for K10 is considerably greater (by a factor of approximately 6) than that for tonsil 13 and that in both cases the majority of the total pore volume is derived from mesopores in the 50–150 Å diameter range. The measured specific surface areas, and total pore volumes for tonsil 13 and K10 are summarised in Table 2.

From Table 2, it can be seen that both the surface area and total pore volume for K10 are considerably greater than for tonsil 13, and by similar factors (five for the surface area and six for the pore volume). This would be consistent with the surface area increase and the creation of the mesoporosity being related phenomena due to the acid treatment procedure. This suggestion is in agreement with the models suggested for the K10 mesoporous structure described above *i.e.* those of Pesquera *et al.*[18] and of Onaka *et al.*[32] From these results it is not clear whether it is likely to be zinc ions residing at surface sites, or zinc ions residing in the mesopores which are the catalytically active species in clayzic, or indeed whether both of these types of ions are catalytically active.

The pore size distribution and cumulative pore volume plots for clayzic are shown alongside the corresponding plots for K10 in Figs. 10 and 11.

Fig. 10 shows that the pore size distribution for clayzic also exhibits an artefact at an apparent diameter of 45 Å. There are significant differences between the pore size distributions for

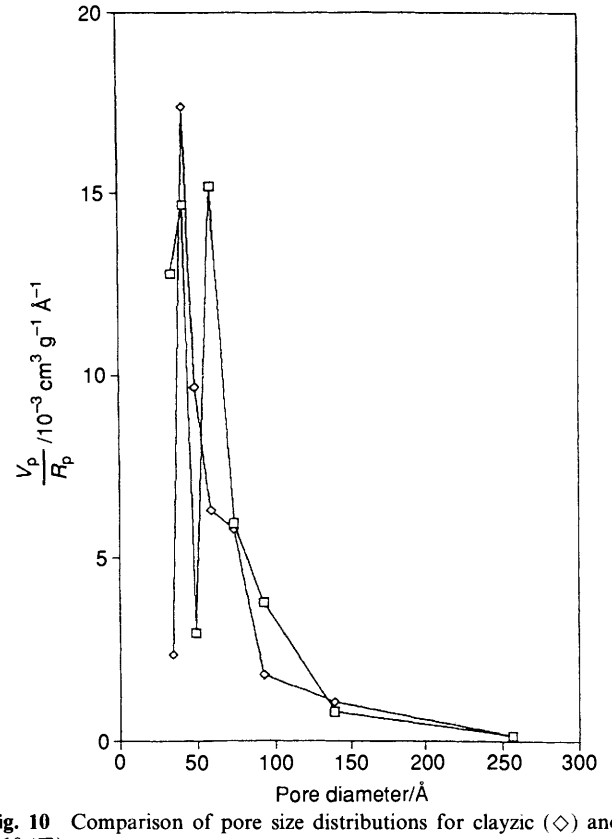

Fig. 10 Comparison of pore size distributions for clayzic (◇) and K10 (□)

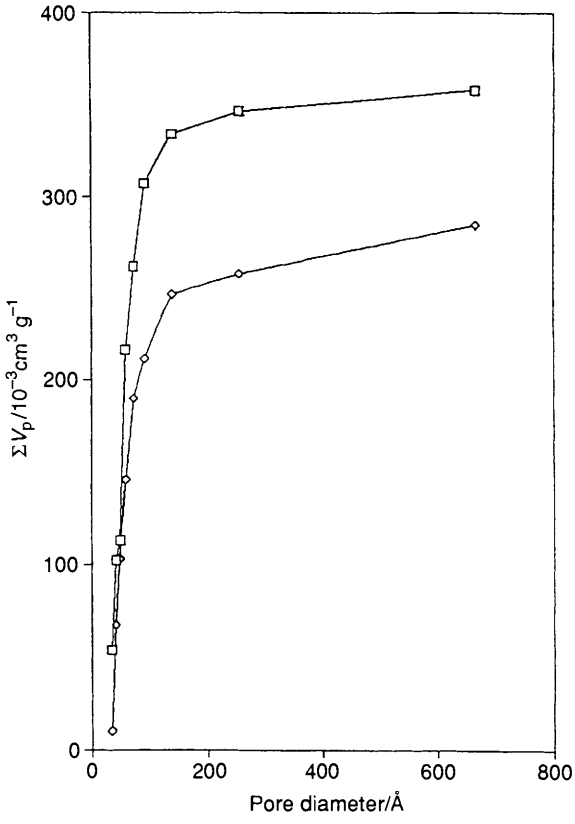

Fig. 11 Comparison of cumulative pore volumes for clayzic (◇) and K10 (□)

K10 and clayzic in the 50–150 Å diameter range. The sharp maximum at about 60 Å in the K10 distribution appears still to be present but is now of much lower intensity, appearing only as a shoulder to the artefact. The broad distribution in the K10 plot between about 70 and 150 Å has been almost totally lost. It seems likely that these changes are a result of zinc incorporation into these pores. It does not seem likely that the appearance of the clayzic distribution arises from 'shrinkage' of the K10 distribution *i.e.* a general shift to lower pore diameter that might be expected if zinc ions were adsorbed on the walls of the pores and the remaining 'core' of the pore were measured. This can be inferred as the shoulder at about 65 Å in the distribution, would have to arise from an increase in the number of pores of about 85 Å diameter (in K10), as well as their filling to reduce the observed pore diameter. That no shrinkage in pore diameter is observed, but that a reduction in the observed number of pores in the 50 to 150 Å diameter range has occurred, implies that either zinc ions fill a proportion of the pores completely, or that pores which contain zinc ions are not observed by the adsorption of dinitrogen. This latter explanation seems reasonable; the surface area of the interlayer regions of montmorillonite clays are known not to be measured by dinitrogen adsorption as they are too polar to allow ingress of the non-polar adsorbate.[24] This would imply that mesopores containing zinc ions are very polar in nature.

The cumulative pore volume plots shown in Fig. 11 show that the measured pore volume for clayzic is considerably lower than that for K10 and that a significant proportion of this volume decrease arises from mesopores in the 50 to 150 Å diameter range. The measured specific surface areas and total pore volumes for K10 and clayzic are given in Table 3.

The data in Table 3 shows that there is a measured total pore volume decrease of 0.08 cm^3 g^{-1} and a measured specific surface area decrease of 98 m^2 g^{-1}, on going from K10 to clayzic. Zinc chloride has a formula weight of 136.28 g mol^{-1} and a density of 2.91 g cm^{-3} at 25 °C. Thus the likely maximum volume that the measured loading of 1.12 mmol g^{-1} could occupy, if all of the supported zinc resides in mesopores, is 0.05 cm^3 g^{-1}. If an average occupied pore has a diameter of 65 Å (32.5 Å pore radius) and a cylindrical pore model is assumed, the maximum surface area decrease, for a pore volume decrease of 0.08 cm^3 g^{-1}, is calculated as 49 m^2 g^{-1}. If an average pore diameter of 100 Å is assumed the maximum surface area decrease is calculated to be 32 m^2 g^{-1}. These calculations lend weight to the hypothesis that mesopores containing significant amounts of zinc irons are not included in the measurements of pore volume (and hence the pore size distribution) and of specific surface area. Thus it seems likely that zinc chloride, when supported on K10, occupies both the surface of the clay and mesopores within the clay and that the pore volume (and hence the contribution to the surface area) of these occupied pores is not measured when using dinitrogen as the adsorbate.

Table 3 Comparison of specific surface area and total pore volume for clayzic and K10

Material	a/m^2 g^{-1}	V_p/cm^3 g^{-1}
K10	230	0.36
Clayzic	132	0.28

If the most active Zn^{2+} sites in clayzic are located in mesopores, it is interesting to note that the measured pore size distribution of clayzic still shows some mesoporosity. From the calculations above, the fact that these pores are detected when using dinitrogen as the adsorbate, might suggest that these pores do not contain significant amounts of zinc ions, *i.e.* that the optimum loading of clayzic might be higher than the 1.12 mmol g^{-1} used here. This loading of clayzic has been used since the original report and was arrived at by analogy with the optimum loading determined for cupric chloride supported on K10 ('Claycuc').[7] Laszlo and co-workers use a zinc chloride

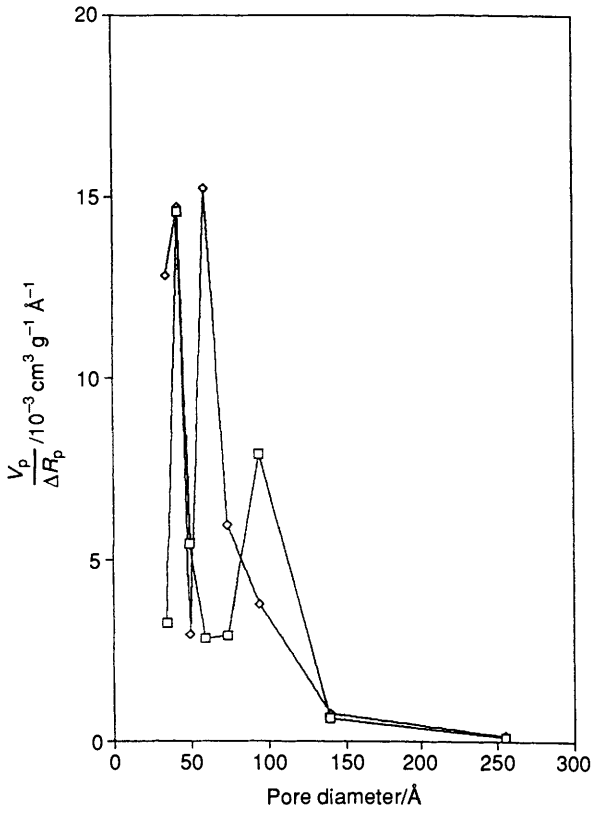

Fig. 12 Comparison of pore size distributions for thermally activated (□) and unactivated (◇) K10

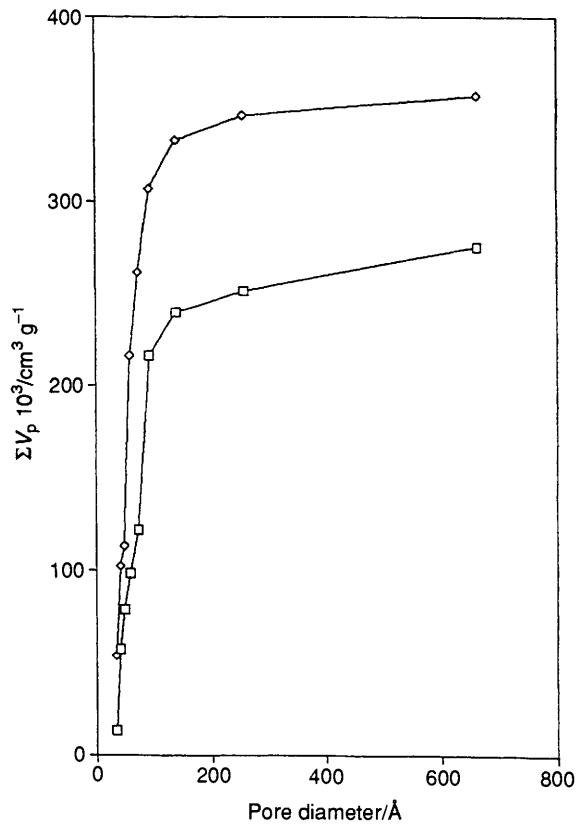

Fig. 13 Comparison of cumulative pore volumes for thermally activated (□) and unactivated (◇) K10

loading of 1.8 mmol g^{-1}, although it is not clear whether this loading has been optimised. Brown and Rhodes have found the optimum loading of zinc for an acid treated form of Carmargo White to be 2.0 mmol g^{-1}.

If the active sites in clayzic do indeed reside in mesopores within the support and supports with pores of about 100 Å diameter provide the most active forms of clayzic, it seems unlikely that the observed selectivity towards *para*-substitution with aromatic substrates[16] arises from physical constraint of the reactants by the support, as has been suggested for reactions occurring in the interlayer regions. One possible contradiction to this argument might be that the pores may have very small openings, *i.e.* that they are of the 'ink bottle' type.[31] This suggestion can be discounted for two reasons: first, in analysing the adsorption data obtained for K10 by the t-plot method of Lippens and De Boer,[34] Pinnavaia found good agreement when using a cylindrical pore shape model;[27] secondly, selectivity towards *para*-substitution of aromatic substrates in constrained systems such as zeolites, can arise from the isomerisation of the *ortho*- and *meta*-substituted products as they are trapped within the structure, or because they have longer diffusion times out of the catalyst. The benzylation of ethylbenzene catalysed by clayzic, has been shown to proceed under non-isomerising conditions.[17]

The pore size distribution and cumulative pore volume for K10 which has been calcined in air at 275 °C (the optimum calcination temperature for catalytic activity of Clayzic)[16] have been determined and are shown in Figs. 12 and 13 respectively. The pore size distribution K10 and cumulative pore volume for unactivated K10 are also shown for comparative purposes.

Fig. 12 shows that calcination in air has a marked effect on the pore size distribution for K10. The pore size distribution plot for calcined K10 unlike unactivated K10 shows relatively little porosity around the 60 Å value, but does show a broad distribution centred around a maximum at about 90 Å. This suggests that the diameters of the mesopores in K10 have been

Table 4 Summary of specific surface area, modal pore diameter (d) and total pore volume data for activated and unactivated K10

Material	a/m^2 g^{-1}	d/Å	V_p/cm^3 g^{-1}
Unactivated K10	230	60	0.36
Calcined K10	200	90	0.28

significantly increased by the calcination procedure and confirms that calcination has a significant structural effect on the support material.

Fig. 13 shows that calcination of K10 at 275 °C overnight actually causes a reduction in the total pore volume of the support. This is surprising, as Fig. 12 shows that the diameters of the mesopores in K10 are increased by calcination. An increase in the average pore diameter of the mesopores in the support, might be expected to cause an increase in the observed total pore volume. However, Fig. 13 is in agreement with the surface area results described earlier, where calcination was observed to cause a reduction in the surface area of K10. The majority of the total pore volume loss observed for thermally activated K10 in Fig. 13, appears to derive from mesopores in the 50–150 Å diameter range. These observations suggest that calcination of K10 may have caused the destruction of some of the mesopores in this range and/or has caused a significant reduction in the average length of these mesopores. These data are summarised in Table 4.

It is possible that calcination at temperatures higher than 275 °C (which has been shown to give rise to lower benzylation reaction rate enhancements than at the optimum temperature)[16] may cause a further shift to higher diameter in the mesopore diameter distribution and/or a further reduction in the total pore volume of the support. Brown and Rhodes have shown that catalysts produced by supporting zinc chloride on mesoporous supports with pore diameters of greater than

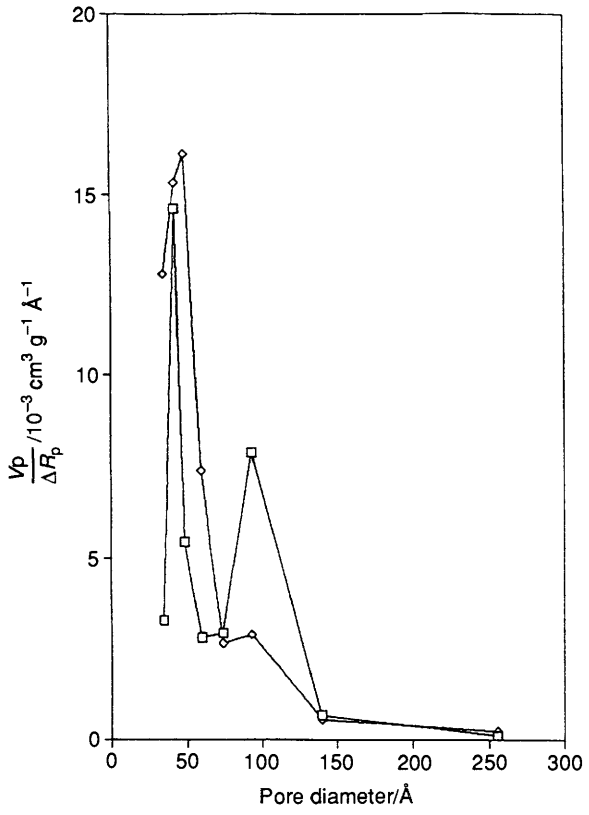

Fig. 14 Comparison of the pore size distributions for activated K10 (□) and activated clayzic (◇)

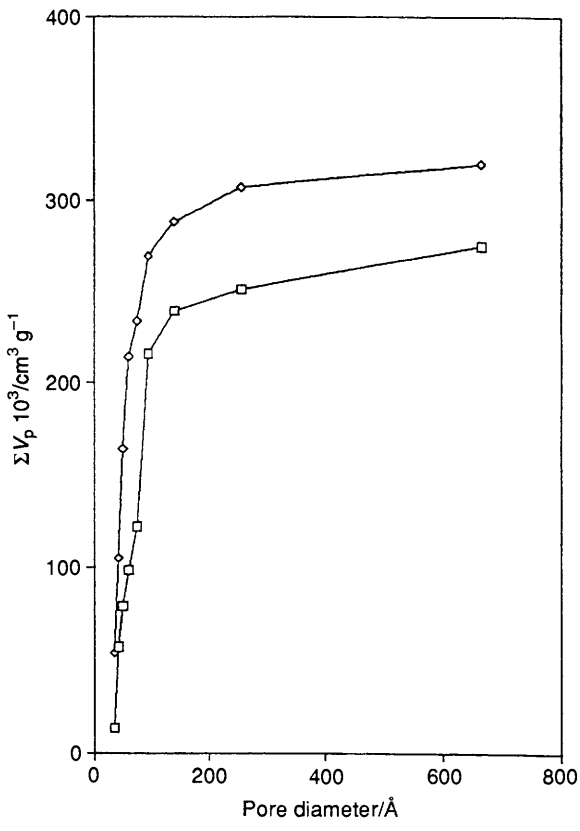

Fig. 15 Comparison of cumulative pore volumes for activated K10 (□) and activated clayzic (◇)

100 Å, results in clayzic-type materials of lower catalytic activity, than those produced from supports with mesopores of 100 Å diameter. The number of mesopores in the support of diameter 100 Å (as would be indicated by the cumulative pore volume plot) would also be expected to have a significant effect on the activity of a clayzic-type material.

The shape of the pore size distribution plot of thermally activated clayzic in Fig. 14 is unexpected. The artefact peak (see earlier) at about 40 Å in the K10 distribution is not present in its expected sharp form and position in the distribution. Instead a broad peak appears between about 30 and 70 Å. Considering the shape of the pore size distribution of thermally activated K10, it seems unlikely that this peak in the distribution actually represents mesoporosity in the 30–70 Å diameter range. It is possible that this peak is due to some macroscopic property of the catalyst caused by the calcination procedure, *i.e.* it is an artefact of a similar nature to that which was expected. The exact cause of this peak cannot be determined with the data available.

The pore size distribution of thermally activated clayzic also shows a peak with a maximum at about 90 Å. This appears to correspond to the broad distribution in the K10 plot, which also has a maximum at about 90 Å, but is of much lower magnitude. This suggests that the pore volumes of those mesopores in this diameter range which contain significant amounts of zinc ions are not measured using dinitrogen as the adsorbate. This is somewhat surprising as the dehydrating effect of the calcination procedure might have been expected to reduce the polarity of the materials. It seems clear that any reduction in polarity is not sufficient to allow ingress of dinitrogen to the mesopores at 77 K.

The cumulative pore volume plot (Fig. 15) for thermally activated clayzic is again unexpected. The calculated total pore volume for thermally activated clayzic is observed to be greater than that for thermally activated K10, despite the former having regions which do not appear to be measured when using dinitrogen as the adsorbate, as was described above. This pore volume effect appears to be caused by the contribution of the broad peak in the pore size distribution of thermally activated clayzic (Fig. 14) and which is likely to be due to an artefact.

Studies on the Active Sites in Clayzic

The acid sites of K10 and clayzic have been investigated by studying the FTIR spectra of the adsorbed probe molecules pyridine and benzonitrile. Pyridine has been shown to be an excellent probe of solid acids, its ring vibration modes are very sensitive to their environment and can be used to differentiate Brönsted acid sites from their Lewis counterparts. Parry has described the use of pyridine as a probe for solid acids.[35]

Pyridine vapour was adsorbed onto samples of K10 and clayzic under vacuum until no further increase in band intensities was observed. Diffuse reflectance FTIR (DRIFT) spectra were then recorded. These are shown in Fig. 16.

The absorption bands in Fig. 16 have been assigned in the following way (after Parry):[35] the bands at 1441 and 1597 cm^{-1} in the K10 spectrum (appearing as shoulders in the clayzic spectrum) are due to vibrations of physisorbed, hydrogen bonded pyridine molecules on the materials' surface. The bands at 1488 cm^{-1} are common to vibrations of physisorbed and coordinatively bound pyridine molecules. The bands at 1537 and 1637 cm^{-1} are due to the formation of the pyridinium ion, produced when pyridine molecules are protonated by Brönsted acid sites. The pyridinium vibration appearing at 1537 cm^{-1} is not due to a ring vibration, but is due to an N^+–H deformation mode. The relative intensities of these bands in the K10 and clayzic spectra suggest that K10 possesses more Brönsted acid sites than clayzic. This implies that some Brönsted acid sites in the support have been destroyed during the formation of clayzic. This does not agree with Laszlo's suggestion that the zinc ions are able to enhance the Brönsted acidity of the system by polarisation of their solvating water molecules.[36] The bands

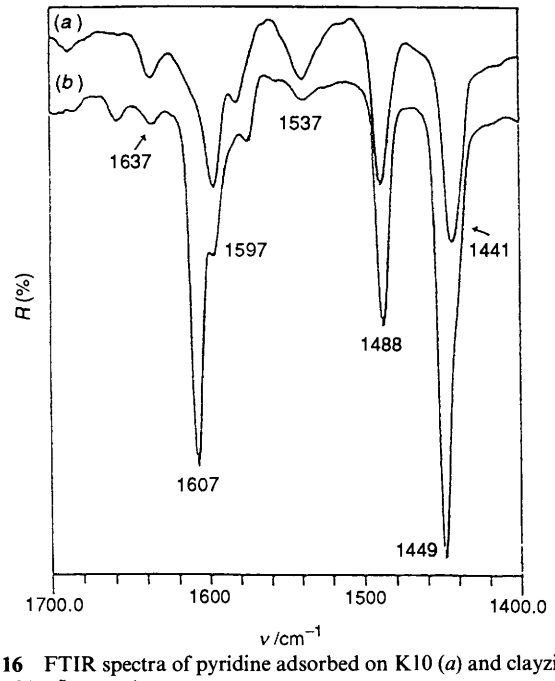

Fig. 16 FTIR spectra of pyridine adsorbed on K10 (*a*) and clayzic (*b*) (*R* = % reflectance)

at 1449 and 1607 cm^{-1} in the spectrum are due to pyridine molecules coordinatively bound to Lewis acid sites. The fact that these bands are only present in the clayzic spectrum suggests that K10 does not possess significant Lewis acidity and that it is the zinc ions in clayzic that are Lewis acidic. The magnitude of the shift in position of these bands (relative to those of hydrogen bonded pyridine in the liquid phase, 1439 and 1582 cm^{-1} respectively) is indicative of the strength of the Lewis acid site. Typically these shifts range between +8 and +21 cm^{-1} for the band at 1439 cm^{-1} in the liquid spectrum and +18 and +48 cm^{-1} for the band at 1582 cm^{-1} in the liquid spectrum. The relatively small shifts of these bands, $\Delta\nu$ = +10 cm^{-1} for the band at 1449 cm^{-1} in the spectrum, and $\Delta\nu$ = +25 cm^{-1} for the band at 1607 cm^{-1} in the clayzic spectrum, suggest that the Lewis acidity of the zinc ions is rather low. This is in agreement with the observed intensities of the pyridinium bands in the clayzic spectrum being lower than those in the K10 spectrum, *i.e.* that the zinc ions are too weakly Lewis acidic to significantly polarise their solvating water molecules sufficiently to protonate pyridine, at ambient temperature and humidity.

The effect of thermal activation on the acid sites of K10 and clayzic has also been investigated using pyridine as an IR probe. Samples of K10 and clayzic were activated in an environmental DRIFT chamber as described above, cooled to ambient temperature and exposed to pyridine vapour until no further increases in the intensities of the pyridine peaks were observed. The spectra obtained are shown in Fig. 17.

Most notably in Fig. 17, the spectra of pyridine adsorbed on thermally activated K10 and clayzic do not show bands at 1540 and 1637 cm^{-1} due to the formation of pyridinium ion and indicative of Brönsted acidity, as were seen in the corresponding spectra for the unactivated samples (Fig. 16). This may be due to the absence of physisorbed water which can be polarised by Lewis acidic cations in the samples after activation. However, the spectrum of pyridine adsorbed on thermally activated K10 like that for unactivated K10 does not show the presence of coordinatively bound pyridine, which would have been indicative of Lewis acidic sites, but only the presence of hydrogen bonded pyridine (bands at 1445 and 1597 cm^{-1}) and the common band at 1490 cm^{-1}. This suggests that the Brönsted acidity in K10 is not due to the polarisation of solvating water by Lewis acidic cations.

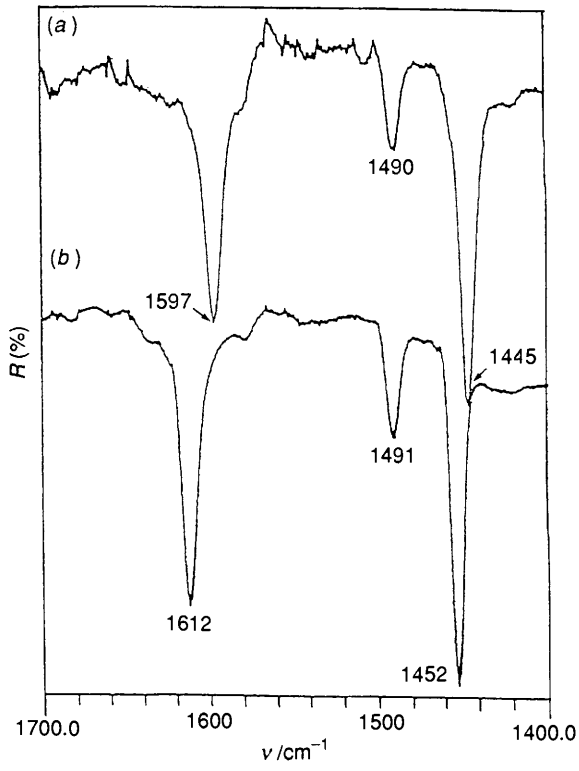

Fig. 17 FTIR spectra of pyridine adsorbed on thermally activated K10 (*a*) and clayzic (*b*)

The spectrum of pyridine adsorbed on thermally activated clayzic does show the presence of coordinatively bound pyridine (bands at 1452 and 1612 cm^{-1}) indicative of Lewis acidic sites (and probably due to the supported zinc ions) in addition to the common band at 1491 cm^{-1}. These bands due to the Lewis acid sites are slightly shifted to higher wavenumber relative to their positions in the spectrum of pyridine adsorbed on unactivated clayzic, although the values of these shifts ($\Delta\nu$ = +3 cm^{-1} for the band at 1452 cm^{-1} and $\Delta\nu$ = +5 cm^{-1} for the band at 1612 cm^{-1}) are probably too small to be significant and certainly do not suggest any significant increase in the activity of individual catalytic sites on thermal activation.

Nitriles have not been extensively employed as probe molecules for solid acids, however they should be selective probes of Lewis acidity, as they are much weaker bases than pyridine and are thus unlikely to be protonated by Brönsted acid sites. They should also only form weak hydrogen bonds. In addition the cyanide stretching vibration is rather sensitive to its environment and quite large shifts should be possible when the cyanide group is coordinated to a Lewis acid site. Coordination to a Lewis acid site is either directly through the formation of a σ-bond to the cyanide nitrogen atom lone pair electrons,[37] or can involve a bridging water molecule.[38] These interactions increase the s-character of the nitrogen atom and hence the bond order of the C≡N group. This increase in bond order causes a shift to higher wavenumber to be observed.[39] Thus the greater the shift in position of the cyanide stretching vibration, the stronger the interaction between the nitrile and the Lewis acid and hence the greater strength of the Lewis acid.[40] The cyanide stretching frequency has been shown to be quite a sensitive probe of the Lewis acidity of a solid, being able to differentiate, the Lewis acidities of Mg^{2+}, Ca^{2+} and Ba^{2+} ions, exchanged into the interlayer regions of a montmorillonite.[38]

Benzonitrile vapour has been adsorbed onto K10 and clayzic under vacuum until no further increase in band intensities was observed. DRIFT spectra were then recorded and are shown in

Table 5 Rates, relative rates, product isomer *para*/*ortho* ratios and substrate Taft π^* and octanol–water partition coefficient data for the clayzic-catalysed benzylation reactions of benzene and a range of alkylbenzenes at 40 °C

Substrate	$k \pm$ sd/h^{-1}	*para*/*ortho* Ratio[a]	k_{ArR}/k_{ArH}	π^*[b]	log k_{ow}[b]
Benzene	0.065 ± 0.004	—	1.00	0.59	2.13
Toluene	1.41 ± 0.03	1.09	21.7	0.55	2.69
Ethylbenzene	0.132 ± 0.006	1.53	2.03	0.53	3.15
Propylbenzene	0.114 ± 0.003	1.49	1.75	0.51	3.66
Cumene	0.059 ± 0.010	3.00[c] (2.01)	0.908	0.51	3.68
Butylbenzene	*d*	*e*	—	0.49	4.26
sec-Butylbenzene	0.078 ± 0.012	3.86[f] (2.36)	1.20	0.49[g]	4.19[g]
tert-Butylbenzene	0.050 ± 0.003	3.85	0.769	0.49	4.11

[a] Numbers in parentheses refer to *para*/(*ortho* + *meta*) ratio. [b] Data at 25 °C. [c] *meta*-Isomer also observed: *o*:*m*:*p*, 22.2:11.0:66.8% = 2.03:1.00:6.08. [d] Rate too slow to be determined with confidence. [e] Small amounts of *meta*-isomer detected. [f] *meta*-Isomer also observed, *o*:*m*:*p*, 22.4:13.5:64.1% = 1.66:1.00:4.75. [g] Estimated as the mean of the values for butyl- and *tert*-butyl-benzene.

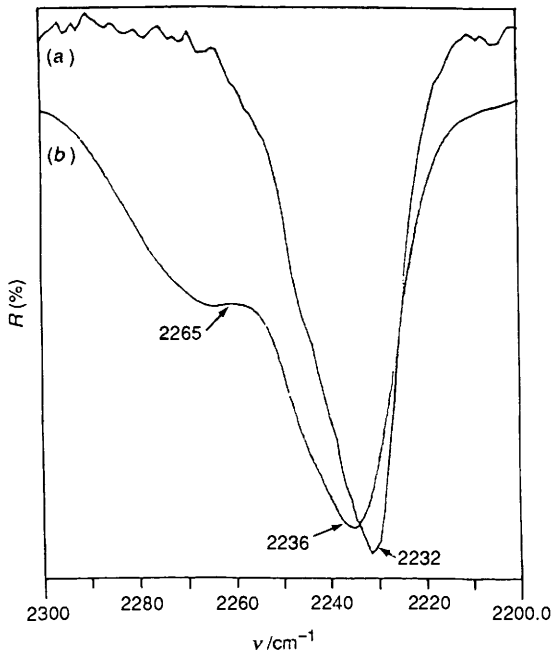

Fig. 18 FTIR spectra of benzonitrile adsorbed on K10 (*a*) and Clayzic (*b*)

Fig. 18. The spectrum of benzonitrile adsorbed on K10 has only one significant band in the cyanide stretching region, at 2232 cm^{-1}. This band shows only a very small shift from the cyanide stretching absorbance of liquid benzonitrile (2229 cm^{-1}, $\Delta\nu$ = +3 cm^{-1}) and is likely to be due to physisorbed, *i.e.* non-bound, or hydrogen bonded, benzonitrile on the support. This suggests that K10 does not have any significant Lewis acidity, in agreement with the results obtained from the pyridine adsorption studies above. The spectrum of benzonitrile adsorbed onto clayzic shows two cyanide stretching vibrations. The band at 2236 cm^{-1} also has a very low shift compared to the cyanide absorbance of liquid benzonitrile ($\Delta\nu$ = +7 cm^{-1}) and is probably due to excess benzonitrile, physisorbed onto the material. The other band, appearing at 2265 cm^{-1} has a relatively large shift compared to the cyanide stretching vibration of liquid benzonitrile ($\Delta\nu$ = +37 cm^{-1}) and is probably due to benzonitrile coordinatively bound to Lewis acid sites. The fact that this band appears in the spectrum of clayzic and not in the spectrum of K10 suggests that it is the zinc ions in clayzic which are responsible for the Lewis acidity. This is in agreement with the results obtained from the pyridine adsorption experiments described above.

The Benzylation of Alkylbenzene using Clayzic

Earlier studies in our laboratory on the relative reactivities of halobenzenes[16] and anisole[12] in clayzic catalysed benzylations have proved to be very revealing in terms of the nature of the active sites and the molecular sieving properties of the catalyst. We have recently turned our attention to alkylbenzenes which are normally considered to be activated substrates in electrophilic aromatic substitutions, compared to benzene and halobenzenes.

The rates, relative rates and mean product isomer distributions for the clayzic catalysed benzylations of a range of alkylbenzenes, compared to benzene, are shown in Table 5. Taft π^* and octanol–water partition coefficient data for the substrates studied are also included.

In assessing these relative reaction rates, it must be assumed that the chemistry which governs the benzylation reaction under homogeneous conditions is still valid under conditions of heterogeneous catalysis, *i.e.* that the rate determining step is the attack of the substrate onto a polarised catalyst–benzyl chloride complex (the electrophile). By studying the clayzic catalysed benzylation of halobenzenes, the rate of this attack has been shown to be limited by the ability of the substrate to enter the polar mesopores containing the active zinc ions.[16] The observed relative rate of reaction is then dependant on the rate at which the substrate attacks and the stability of the Wheland intermediate formed in the rate determining step.

The relative rates for toluene, ethylbenzene, propylbenzene and cumene appear to largely follow a hyperconjugative ability trend, *i.e.* toluene (3 α-C–H) > ethylbenzene (2) ≈ propylbenzene (2) > cumene (1). The observed relative reactivity of cumene is unexpected. Cumene would have been expected to show a slower relative reactivity than propylbenzene (as it has one less α-C–H proton with which to stabilise the Wheland intermediate by hyperconjugation), which is indeed observed, but still show a reactivity higher than that of benzene (due to the stabilising +I effect of the alkyl substituent), which is not. The observed reactivities of butyl- and *tert*-butyl-benzene are also unexpectedly slower than of benzene. The observed relative reactivities within the butylbenzene series are also unexpected from hyperconjugative and steric hindrance considerations. In addition, all of the relative reactivities of the higher alkylbenzenes are slower than would have been expected on the basis of the relative reactivity of toluene. These effects could be explained by differences in the abilities of the substrates to enter the polar mesopores containing the active zinc ion centres, as was seen for the halobenzenes.[16]

The Taft π^* values for the alkylbenzenes are all similar and relatively low compared to benzene and the halobenzenes. The alkylbenzenes would be expected to have small dipole moments and be largely non-polarisable. Substrate polarisability was

Table 6 Calculated pseudo-first order reaction rate constants, *para*/*ortho* isomer ratios and relative reaction rates for the benzylation of benzene and some alkylbenzenes, catalysed by thermally activated clayzic at 40 °C

Substrate	$k \pm$ sd/h^{-1}	*para*/*ortho* Ratio[a]	k_{ArR}/k_{ArH}	$k_{thermal}/k_{unactivated}$
Benzene	2.01 ± 0.25	—	1.00	30.8
Toluene	59.0 ± 9.0	1.33	29.3	41.8
Ethylbenzene	2.74 ± 0.50	1.66	1.18	18.0
Propylbenzene	5.47 ± 0.55	1.63	2.72	48.0
Cumene	42.0 ± 7.6	3.10[b] (2.11)	20.9	712
Butylbenzene	0.286 ± 0.038	1.66[c]	0.14	*e*
sec-Butylbenzene	0.998 ± 0.267	4.30[d] (2.55)	0.50	12.8
tert-Butylbenzene	11.0 ± 2.3	4.15	5.48	220

[a] Numbers in parentheses refer to *para*/(*ortho* + *meta*) ratio. [b] *meta*-Isomer also observed: *o*:*m*:*p*, 22.0:10.2:67.8% = 2.15:1.00:6.64. [c] Small amounts of *meta*-isomer detected. [d] *meta*-Isomer also observed, *o*:*m*:*p*, 16.8:11.2:72.0% = 1.50:1.00:6.45. [e] Rate of reaction catalysed by unactivated clayzic was too slow to be measured with confidence, therefore ratio cannot be calculated.

identified as being important to the abilities of the halobenzenes to enter the polar pores of clayzic.[16] Better correlation is obtained between the observed relative reactivities of the alkylbenzenes and their octanol–water partition coefficients, than with their Taft π^* values. This could be a consequence of the low polarisabilities of the alkylbenzenes. The values for the octanol–water partition coefficients of the alkylbenzenes vary by a factor of 38 and could partly account for the observed differences in observed reaction rates. For example the small relative rate enhancement of *sec*- over *tert*-butylbenzene could be accounted for by considering the rate enhancing effect of the one α-C–H proton in *sec*-butylbenzene against the rate retarding effect of the (estimated) higher octanol–water partition coefficient of this substrate.

The observed differences in mean product isomer distributions must be explained by the effects of the alkyl substituent on the substrates, as a common electrophile can be assumed to be produced in each case. The calculated mean product isomer ratios appear to follow a similar steric hindrance trend to that observed by Olah for $AlCl_3$ catalysed benzylations.[39,41] This can be seen if the mean *para*/(*ortho* + *meta*) ratios for cumene and *sec*-butylbenzene are considered, although the mean *para*/*ortho* ratio for propylbenzene appears to be out of step.

Strangely, *meta*-substituted product isomers are only observed for cumene and butyl- and *sec*-butyl-benzenes. It would have been expected that all the substrates investigated would produce *meta*-substituted products to some extent if the catalyst produced isomerising conditions (as in the case for $AlCl_3$-catalysed reactions,[42] for example). The calculated mean *para*/*ortho* ratios for cumene and *sec*-butylbenzene are higher than expected from steric hindrance considerations, although their mean *para*/(*ortho* + *meta*) ratios do agree with this theory, as was discussed above. These observations suggest that the *meta*-substituted products are produced largely from the *ortho*-substituted product. This agrees with the results of Condon, obtained under $AlCl_3$-catalysed isomerising conditions.[42] The observation of *meta*-substituted products cannot be explained from purely steric considerations, as no *meta*-isomer is produced from the benzylation of *tert*-butylbenzene. The only immediately obvious difference between cumene, *sec*- and *tert*-butylbenzenes is that the latter substrate cannot stabilise the Wheland intermediate by hyperconjugation of an α-C–H proton. The production of the *meta*-substituted products is unlikely to arise from isomerisation of the alkyl substituent. If this had been the case, *tert*-butylbenzene would have been expected to show the greatest level of migration and the *sec*-butyl group might have been expected to partially isomerise to the more stable *tert*-butyl group. Neither of these phenomena were observed. Overall, these results suggest that isomerisation of the benzyl group, from the *ortho*- to the *meta*-position, occurs in the benzylation of alkylbenzenes that have bulky alkyl substituents that can stabilise the Wheland intermediate by hyperconjugation.

The effect of thermal activation of clayzic (by calcination in air at 275 °C overnight and cooling over phosphorous pentoxide) on the benzylation of benzene and some alkylbenzenes and anisole at 40 °C has also been investigated. Calculated pseudo-first order reaction rates, relative rates (to benzene and to the corresponding reactions catalysed by unactivated, Table 5) and *para*/*ortho* product isomer ratios determined for these reactions are summarised in Table 6.

The calculated relative reaction rates (relative to the corresponding reactions catalysed by unactivated clayzic) again show that considerable rate enhancements can be achieved by thermally activating the catalyst at the optimum calcination temperature of 275 °C. Rate enhancements were also observed with the halobenzenes[16] but the effect is more pronounced with the alkylbenzenes. This is probably because the partitioning of the alkylbenzenes into the mesoporous catalyst before activation is likely to be very low and lower than that of the halobenzenes or even benzene (as is shown by the octanol–water partition coefficients, Table 5). The explanation for the extremely high rate enhancements seen for the benzylations of cumene and *tert*-butylbenzene is not clear.

The observed relative reaction rates (to benzene) again appear generally to arise from a combination of electronic effects and the ability of the substrate to enter the polar mesopores, in order to combine with the electrophile in the rate determining step. However, not all of the alkylbenzene reactions show reaction rates higher than that for benzene, which would be expected in, for example, an homogeneous system. This implies that partitioning of the substrate into the catalyst structure still has a considerable influence on the observed reactivity of the system.

Comparison of the observed *para*/*ortho* product isomer ratios (Table 6) with those obtained when using unactivated clayzic as the catalyst (Table 5) shows that in each case the thermally activated catalyst is more selective towards the *para*-substituted isomer. This is in agreement with the results obtained for the halobenzenes[16] and further suggest that thermally activated clayzic produces a weaker (and thus more selective) electrophile. This would suggest that the mean effective strength of the active sites has been diminished by the calcination procedure and that it is an increase in turnover efficiency which is responsible for the observed enhancements in observed rate.

Concluding Remarks

The successful extension of the use of supported reagents from stoichiometric reagents to genuine catalytic materials in liquid

phase organic reactions is an extremely important development both in the context of supported reagent chemistry and is the development of new 'cleaner' chemical methods and processes.

Friedel–Crafts chemistry is a particularly important area of organic chemistry and industrial chemistry in this context and the exploitation of solid acid catalysts such as clayzic is of growing importance.

Clayzic is a very effective catalyst for Friedel–Crafts alkylations. It is a rather complex material being based on an acid treated montmorillonite which has little residual lamellar structure. It appears that clayzic is essentially amorphous with its activity being largely due to a high local concentration of Zn^{2+} ions contained in structural mesopores rather than a surface area effect. Individual zinc sites do not show particularly high Lewis acidity and there is no evidence for significant Brönsted acidity. The presence of water in the mesopores greatly increases the local polarity with important consequences for the measured surface area and pore volume distribution and on the relative reactivities of aromatic substrates towards benzylation.

The successful exploitation of a new catalyst can only be realised by achieving a reasonable understanding of its nature and the origin of its activity. For many years supported reagent chemistry has largely relied on serendipity. Spectroscopic studies on supported cyanides and other stoichiometric materials demonstrated the importance of optimising the loading, choice of support, *etc.* Spectroscopic and other studies on supported fluorides for example, have helped us to understand the unexpected and surprisingly complex behaviour of the materials. The discovery of clayzic was largely serendipitous and it is again only through detailed, multi-technique, analysis that the secrets of its activity are beginning to be revealed.

Supported reagents can no longer be considered as simply being high surface area forms of the reagent. The structure of the support, the location and nature of the active sites and the synergism between support and reagent can all be important factors. After over 20 years as academic curiosities relying mostly on serendipitous discoveries, supported reagents now seem set for a promising future in organic and industrial chemistry.

Experimental

Powder XRD patterns of clay samples (deposited from aqueous suspensions onto glass slides and allowed to dry under ambient conditions overnight) were recorded on a Philips 1050 diffractometer using Cu-Kα radiation. We gratefully acknowledge Dr. D. R. Brown for making this equipment available.

Cation exchange capacities (CECs) were determined photometrically by comparing the UV–VIS absorption at 663 nm of an aqueous solution of methylene blue before and after mechanical shaking with a known mass of clay for 20 min, by analogy with the method of Robertson and Ward.[20] The clay was removed from the solution by filtration through cotton wool (which was shown not to adsorb the dye) to prevent scattering of the incident radiation by residual particulate matter.

Specific surface areas and porosity data were determined by adsorption of dinitrogen at 77 K [surface areas being calculated by application of the Brunauer, Emmett and Teller (BET) isotherm], using a Quantachrome Corporation, 'Quantasorb' surface area analyser and linear mass flow controller.

DRIFT spectra were recorded of powder samples (diluted with KBr) using a Perkin-Elmer 1720 FTIR spectrometer, equipped with a Specac environmental diffuse reflectance chamber. This environmental chamber was connected to a vacuum line system to allow the addition of probe molecules as vapours.

The benzylation of the alkylbenzenes was performed by adding 0.5 mol of substrate (Aldrich, >99% purity, dried over 3 Å molecular sieves) to 2.00 g of clayzic (either unactivated or activated by calcining in air at 275 °C overnight and cooling to ambient temperature over P_2O_5 in a desiccator) and heating of the mixture with stirring to 40 °C. Benzyl chloride (0.1 mol) (Aldrich >99% purity) was then added in one aliquot and the progress of the reaction was monitored by following the consumption of benzyl chloride with time, by GC (response factor corrected) and pseudo-first-order reaction rates were calculated on this basis. Isomer ratios of the monobenzylated products were determined from the respective GC peak areas and are uncorrected.

Acknowledgements

Our research on supported reagent chemistry would not have been possible without the generous support of Contract Chemicals Ltd., the Teaching Company Scheme and the SERC. The ideas and guidance of many academic and industrial colleagues have also been invaluable including Jack Miller, Brian Trenbirth, Keith Martin, Adrian Kybett and Chris Brown. Finally, and most importantly, special thanks are due to past and current members of the J.H.C. Research Group and the Envirocats Project Team.

References

1 T. W. Bastock and J. H. Clark, in *Speciality Chemicals*, Elsevier, London, 1991.
2 P. Laszlo, ed., *Preparative Chemistry using Supported Reagents*, Academic, San Diego, 1987.
3 K. Smith, ed., *Solid Supports and Catalysts in Organic Synthesis*, Ellis Horwood, Chichester, 1992.
4 J. H. Clark, A. P. Kybett and D. J. Macquarrie, *Supported Reagents: Preparation, Analysis and Applications*, VCH, New York, 1992.
5 Eur. Pat., 1989, 89303434.
6 A. A. Al Jazzaa, J. H. Clark and M. S. Robertson, *Chem. Lett.*, 1982, 405.
7 J. H. Clark, A. P. Kybett, D. J. Macquarrie, S. J. Barlow and P. Landon, *J. Chem. Soc., Chem. Commun.*, 1989, 1353.
8 Eur. Pat. Appl., 1989, 89303433.
9 B. E. M. Hassan, E. A. Sultan, F. M. Tawfik and S. M. Sappah, *Egypt J. Chem.*, 1985, **28**, 93.
10 P. Laszlo and A. Mathy, *Helv. Chim. Acta*, 1987, **70**, 577.
11 J. H. Clark, A. P. Kybett, M. J. Darby, S. J. Barlow, P. Landon and K. Martin, *J. Chem. Res. (S)*, 1991, 74.
12 S. J. Barlow, T. W. Bastock, J. H. Clark and S. R. Cullen, *Tetrahedron Lett.*, 1993, **34**, 3399.
13 A. Cornélis, C. Dony, P. Laszlo and K. M. Nsunda, *Tetrahedron Lett.*, 1991, **32**, 2903.
14 C. N. Rhodes, M. Franks, G. M. B. Parkes and D. R. Brown, *J. Chem. Soc., Chem. Commun.*, 1991, 804.
15 C. N. Rhodes and D. R. Brown, *J. Chem. Soc., Faraday Trans.*, 1992, **88**, 2269.
16 J. H. Clark, S. R. Cullen, S. J. Barlow and T. W. Bastock, *J. Chem. Soc., Perkin Trans. 2*, 1994, 411.
17 S. R. Cullen, D.Phil. Thesis, University of York, UK, 1994.
18 C. Pesquera, F. Gonzalez, I. Benito, C. Blanco, S. Mendioroz and J. Pajones, *J. Mol. Chem.*, 1992, **2**, 907.
19 *Crystal Structures of Clay Minerals and their X-Ray Identification*, Mineralogical Society, Monograph No. 5, eds. G. W. Brindley and G. Brown, Mineralogical Society, 1988.
20 R. H. S. Robertson and R. M. Ward, *J. Pharm. Pharmcol.*, 1951, **5**, 27.
21 R. W. McCabe, personal communication.
22 P. Laszlo, *Recherche*, 1990, **219**, 314.
23 C. N. Rhodes and D. R. Brown, *J. Chem. Soc., Faraday Trans.*, 1993, **89**, 1387.
24 F. Krachenbuchl, W. I. Stoeckli, J. Brunner, G. Kahr and M. Mueller-Von Mous, *Clay Miner.*, 1989, **32**, 1.
25 A. Cornélis, P. Laszlo and S. F. Wang, *Catal. Lett.*, 1993, **7**, 63.
26 T. H. Milliken, A. G. Oblad and G. A. Mills, *Bull. Clay Miner. Soc.*, 1955, No. 169, 314.
27 J. P. Butrille and T. J. Pinnavaia, *Catal. Today*, 1992, **14**, 141.
28 S. Brunauer, L. S. Deming, W. J. Deming and E. Teller, *J. Am. Chem. Soc.*, 1940, **62**, A23.

29 S. J. Gregg and K. S. W. Sing, *Adsorption, Surface Area and Porosity*, Academic Press, London, 1992.
30 K. S. W. Sing, D. H. Everett, R. A. W. Haul, L. Moscou, R. A. Pierotti, J. Couquerol and T. Siemienewska, *Pure. Appl. Chem.*, 1985, **57**, 603.
31 J. H. De Boer, in *The Structure and Properties of Porous Material*, eds. D. H. Everett and F. S. Store, Butterworth, London, 1958.
32 M. Onaka, T. Shidan, Y. Izumi and E. Nocen, *Chem. Lett.*, 1993, 117.
33 P. Laszlo, *Pure Appl. Chem.*, 1990, **62**, 2027.
34 J. H. De Boer, D. C. Lippens, B. G. Linsen, J. C. P. Broekhoff, A. Van Der Heuval and Th. J. Oniga, *J. Colloid Interface Sci.*, 1966, **21**, 405.
35 G. P. Patty, *J. Catal.*, 1963, **2**, 371.
36 A. Cornélis, P. Laszlo and S. F. Wang, *Tetrahedron Lett.*, 1993, **34**, 3849.
37 S. G. Yim, P. H. Son and K. Kim, *J. Chem. Soc., Faraday Trans.*, 1993, **89**, 837.
38 J. M. Serratosa, *Am. Mineral.*, 1968, **53**, 1244.
39 K. F. Purcell and R. S. Drago, *J. Am. Chem. Soc.*, 1966, **88**, 919.
40 Y. I. Taracevich and F. P. Orcharenko, *Proc. Int. Clay. Conf.*, 1972, 627.
41 G. A. Olah and S. Flood, *J. Am. Chem. Soc.*, 1962, **84**, 1688.
42 F. Condon, *J. Am. Chem. Soc.*, 1948, **70**, 2263.

Paper 4/01218F
Received 28*th February* 1994
Accepted 21*st March* 1994